Table III. Selected Bond Distances (Å) and Interbond Angles (deg) for $[cpFeIrCl_2(PMe_2Ph)(MeN(PF_2)_2)_2]$

molecule 1		molecule 2	
	Bond Distances		
Ir(1)-Fe(1)	2.838 (2)	Ir(2)-Fe(2)	2.828 (2)
Ir(1)-P(1)	2.162 (4)	Ir(2)-P(9)	2.165 (3)
Ir(1)-P(3)	2.151 (4)	Ir(2)-P(6)	2.170 (3)
Ir(1)-P(5)	2.401 (3)	Ir(2)-P(10)	2.409 (3)
Ir(1)-Cl(1)	2.420 (4)	Ir(2)-Cl(4)	2.432 (3)
Ir(1)-Cl(2)	2.422 (4)	Ir(2)-Cl(3)	2.417 (3)
Fe(1)-P(2)	2.050 (6)	Fe(2)-P(8)	2.054 (4)
Fe(1)-P(4)	2.047 (4)	Fe(2)-P(7)	2.061 (4)
Fe(1)-C(13)	2.09 (2)	Fe(2)-C(29)	2.11 (2)
Fe(1)-C(14)	2.06 (2)	Fe(2)-C(30)	2.09 (2)
Fe(1)-C(15)	2.07 (2)	Fe(2)-C(26)	2.06 (2)
Fe(1)-C(16)	2.12 (2)	Fe(2)-C(27)	2.09 (2)
	Interbond Angles		
Fe(1)-Ir(1)-P(1)	89.4 (1)	Fe(2)-Ir(2)-P(9)	87.9 (1)
Fe(1)-Ir(1)-P(3)	88.3 (1)	Fe(2)-Ir(2)-P(6)	86.6 (1)
Fe(1)-Ir(1)-P(5)	171.11 (9)	Fe(2)-Ir(2)-P(10)	171.78 (9)
Fe(1)-Ir(1)-Cl(1)	88.3 (1)	Fe(2)-Ir(2)-Cl(4)	92.4 (1)
Fe(1)-Ir(1)-Cl(2)	90.0 (1)	Fe(2)-Ir(2)-Cl(3)	88.4 (1)
P(1)-Ir(1)-P(3)	94.2 (1)	P(9)-Ir(2)-P(6)	94.3 (1)
P(1)-Ir(1)-P(5)	98.1 (1)	P(9)-Ir(2)-P(10)	97.3 (1)
P(1)-Ir(1)-Cl(1)	85.0 (2)	P(9)-Ir(2)-Cl(4)	87.7 (1)
P(1)-Ir(1)-Cl(2)	176.7 (2)	P(9)-Ir(2)-Cl(3)	176.1 (1)
P(3)-Ir(1)-P(5)	95.9 (1)	P(6)-Ir(2)-P(10)	98.4 (1)
P(3)-Ir(1)-Cl(1)	176.5 (1)	P(6)-Ir(2)-Cl(4)	177.9 (1)
P(3)-Ir(1)-Cl(2)	89.1 (1)	P(6)-Ir(2)-Cl(3)	86.4 (1)
P(5)-Ir(1)-Cl(1)	87.6 (1)	P(10)-Ir(2)-Cl(4)	81.4 (1)
P(5)-Ir(1)-Cl(2)	82.2 (1)	P(10)-Ir(2)-Cl(3)	86.4 (1)
Cl(1)-Ir(1)-Cl(2)	91.8 (2)	Cl(4)-Ir(2)-Cl(3)	91.6 (1)
Ir(1)-Fe(1)-P(2)	89.4 (2)	Ir(2)-Fe(2)-P(8)	90.2 (1)
Ir(1)-Fe(1)-P(4)	90.1 (1)	Ir(2)-Fe(2)-P(7)	90.3 (1)
Ir(1)-Fe(1)-C′[a]	132.5	Ir(2)-Fe(2)-C″[a]	121.5
P(2)-Fe(1)-P(4)	95.6 (2)	P(8)-Fe(2)-P(7)	96.7 (2)
P(2)-Fe(1)-C′	123.8	P(8)-Fe(2)-C″	127.1
P(4)-Fe(1)-C′	124.5	P(7)-Fe(2)-C″	121.4

[a] C′ or C″ is the centroid of the cyclopentadienyl ring.

the rather long metal–metal distance, although there are no structural criteria that can be applied to unequivocally distinguish between them. We do note that the metal–metal distance is slightly *longer* than the intraligand P---P separation (2.787 (5)–2.816 (6) Å), suggesting that the metal–metal interaction is not strong. Considering the iridium to be formally Ir(III) is also consistent with the most unusual feature of **1**, namely the net transfer of a chlorine ligand from iron to iridium that has occurred during the synthesis. While extensive mechanistic speculation is unwarranted, it is tempting to suggest that this occurs via formal oxidative addition of the Fe–Cl bond to the original Ir(I) center, most likely following initial attachment of the fluorophosphine ligand(s).

The Ir–Cl distances compare well with those trans to phosphorus in *mer*- and *fac*-$[IrCl_3(PMe_2Ph)_3]$[21] (2.434 (1)–2.468 (2) Å), while the Ir–PMe_2Ph distances are somewhat longer than those trans to phosphorus in *mer*-$[IrCl_3(PMe_2Ph)_3]$ (2.363 (1)–2.384 (1) Å)[21] and *mer*-$[IrCl_2(H_2O)(PMe_2Ph)_3]ClO_4$ (2.366 (3), 2.392 (3) Å).[22] They are, however, quite comparable to two of the Ir–P distances in *trans*-$[IrCl_2(PMe_2Ph)_4]ClO_4$ (2.416 (1), 2.424 (2) Å).[23] Clearly these long distances reflect a significant trans influence of the Fe–Ir interaction but do not permit a distinction between the two possible descriptions noted above.

Acknowledgment. Support from the Tulane University Chemistry Department and Pennzoil Corp. is gratefully acknowledged.

Registry No. 1, 131067-38-4; 2, 131067-39-5; 3, 131067-40-8; $[Ir(CO)Cl(PMe_2Ph)_2]$, 22685-99-0; $[RhCl(CO)_2]_2$, 14523-22-9; $[CpFeCl(MeN(PF_2)_2)_2]$, 64387-50-4.

Supplementary Material Available: Figures showing the conformations of the two independent molecules of **1**, together with tables of nonessential interatomic distances, interbond angles, calculated hydrogen atom positions, anisotropic thermal parameters, rms amplitudes of anisotropic displacement, and torsion angles (19 pages); a table of observed and calculated structure factors (40 pages). Ordering information is given on any current masthead page.

(21) Robertson, G. B.; Tucker, P. A. *Acta Crystallogr.* **1981**, *B37*, 814.
(22) Deeming, A. J.; Proud, G. P.; Dawes, H. M.; Hursthouse, M. B. *J. Chem. Soc., Dalton Trans.* **1986**, 2545.
(23) Deeming, A. J.; Doherty, S.; Marshall, J. E.; Powell, N. I. *J. Chem. Soc., Chem. Commun.* **1989**, 1351.

Photochemical Reaction of a Diplatinum μ-Phenylethenylidene Complex with Diphenylacetylene: Unusual Formation of a μ-η^1:η^3-Butadienediyl Complex

Eduardo Baralt,[1a] Charles M. Lukehart,*[1a] Andrew T. McPhail,*[1b] and Donald R. McPhail[1b]

Departments of Chemistry, Vanderbilt University, Nashville, Tennessee 37235, and Duke University, Durham, North Carolina 27706

Received June 4, 1990

Summary: Photochemical reaction of a diplatinum μ-alkenylidene complex with PhC≡CPh occurs with C–C coupling of the alkenylidene and alkyne moieties to give an expanded, unsaturated μ-η^1:η^3-butadienediyl ligand. Structural and isotopic-labeling studies indicate that this reaction proceeds by an unusually complex mechanism.

We reported recently that the cationic diplatinum μ-phenylethenylidene complex $[Pt_2(\mu\text{-}C{=}CHPh)(C{\equiv}CPh)(PEt_3)_4][BF_4]$ (1) exhibits pronounced photochemical reactivity reminiscent of that of the well-studied anionic diplatinum complex $[Pt_2(P_2O_5H_2)_4]^{4-}$, even though these two compounds are structurally dissimilar.[2] For example, complex 1 reacts under photolysis with methyl iodide to give analogous neutral diplatinum iodide or diiodide compounds or with 2-propanol to give catalytic production of

(1) (a) Vanderbilt University. (b) Duke University.

(2) Baralt, E.; Boudreaux, E. A.; Demas, J. N.; Lenhert, P. G.; Lukehart, C. M.; McPhail, A. T.; McPhail, D. R.; Myers, J. B., Jr.; Sacksteder, L. A.; True, W. R. *Organometallics* **1989**, *8*, 2417-2430.

0276-7333/91/2310-0516$02.50/0

acetone and molecular hydrogen. Both reactions indicate photolytic atom-transfer reactivity. Furthermore, several halide derivatives of **1** have been characterized as luminescent molecules.

We now report that **1** reacts photochemically with diphenylacetylene to effect C–C coupling of the μ-alkenylidene and alkyne moieties to give an expanded, unsaturated μ-η^1:η^3-butadienediyl ligand. Such C–C coupling reactions are not known for $[Pt_2(P_2O_5H_2)_4]^{4-}$ to our knowledge.[3] Structural and isotopic-labeling studies indicate that this reaction proceeds by a mechanism involving an unusual group-transfer rearrangement. The only other known formation of a μ-η^1:η^3-butadienediyl complex to our knowledge is that reported by Casey and co-workers.[4] In their system, a diiron μ-η^1:η^3-butadienediyl complex is formed under photolysis from a metallacyclopentenone precursor, and a similar group-transfer rearrangement is not apparently operative in this system.

Several related *mononuclear* compounds containing η^3-butadienyl ligands have been prepared by a variety of methods, including rearrangement of a Pt(η^2-cyclopropenyl) compound by Hughes and co-workers,[5] rearrangement of η^1-cyclobutenyl complexes of Ru or W by Bruce and co-workers,[6] dehydrochlorination of a Re(η^3-allyl) compound by Herrmann and co-workers,[7] deprotonation of a cationic Mo(η^4-pentadiene) complex of fluoride-induced desilylation of a cationic Mo(η^4-pentadiene) complex by Green and co-workers,[8] rearrangement of Fe(η^1-perfluorobutadienyl) compounds by Nesmeyanov and co-workers,[9] and reaction of $[Mo(bpy)(CO)_3Cl]^-$ with 1,4-dichlorobut-2-yne either in wet methanol or in the presence of primary or secondary aliphatic amines by Brisdon and co-workers.[10]

Experimental Section

Materials and Methods. All reactions were performed under dry, prepurified nitrogen. General procedures for solvent purification and for acquiring spectroscopic data have been published previously.[11] ^{13}C NMR spectra were recorded on an IBM NR-200 spectrometer operating at a frequency of 50.3 MHz. Chemical shifts were measured with respect to the internal reference of Me_4Si in $CDCl_3$. Microanalyses were performed by Galbraith Laboratories, Inc., Knoxville, TN.

Complex **1** was prepared according to the published procedure.[12] Diphenylacetylene and phenylacetylene-2-^{13}C were used as obtained from commercial sources.

Table I. Crystallographic Data for Complex 2

mol formula	$C_{54}H_{81}BF_4P_4Pt_2$
fw	1331.13
cryst syst	triclinic
space group	$P\bar{1}(C_i^1)$, No. 2
a, Å	15.290 (2)
b, Å	16.927 (2)
c, Å	13.035 (2)
α, deg	100.19 (1)
β, deg	114.85 (1)
γ, deg	71.52 (1)
no. of orientation rflns; θ range, deg	25; 29–38
V, Å^3	2900 (1)
Z	2
D_{calcd}, g cm^{-3}	1.524
μ(Cu Kα radiation, λ = 1.5418 Å)	104.1
temp, °C	25
cryst dimens, mm	0.06 × 0.08 × 0.12
T_{max}:T_{min}	1.00:0.80
scan type	ω–2θ
scan width, deg	0.90 + 0.14 tan θ
θ_{max} deg	62
intens control rflns; variation; repeat time, h	223, $\overline{223}$; <2%; 2
total no. of rflns (+h,±k,±l) recorded	9553
no. of nonequiv rflns recorded	9098
R_{merge} (on I)	0.030
no. of rflns retained (I > 3.0$\sigma(I)$)	4647
no. of params refined	591
extinction cor	2.2 × 10^{-7}
GOF[a]	1.1
R (R_w)[a]	0.040 (0.046)
max shift:esd in final least-squares cycle	<0.02 for Pt, P, C; <0.7 for B, F
final $\Delta\rho$ max, min, e Å^{-3}	+0.60, −0.63

[a] $R = \sum||F_o| - |F_c||/\sum|F_o|$; $R_w = \sum w(|F_o| - |F_c|)^2/\sum w|F_o|^2)^{1/2}$; $\sum w\Delta^2$ ($w = 1/\sigma^2(|F_o|)$, $\Delta = |F_o| - |F_c|$) was minimized; GOF = $[\sum w\Delta^2/(N_{observns} - N_{params})]^{1/2}$.

Preparation of [Pt(PEt$_3$)$_2${μ-η^1:η^3-C(Ph)(H)C(Ph)C≡C-(Ph)}Pt(PEt$_3$)$_2$(C≡CPh)][BF$_4$] (2). To a stirred solution of 0.10 mmol of $[Pt_2(\mu\text{-}C{=}CHPh)(C{\equiv}CPh)(PEt_3)_4][BF_4]$ (**1**) in 10 mL of CH_2Cl_2 was added 0.11 mmol of PhC≡CPh. The reaction solution was degassed in a Pyrex glass vessel of 1-mm thickness (which was fitted with a cold finger to maintain a reaction temperature of 16 °C) by applying a sparge for 5 min. The solution was irradiated with 100-W Hanovia medium-pressure mercury lamp under vigorous stirring. After 8 h, the solution had changed color from orange-red to yellow. The solution was chromatographed through alumina (in a Schlenk frit), and a yellow band was eluted with THF. The solvent was removed under reduced pressure. The yellow residue was crystallized from CH_2Cl_2/*n*-hexane (1:6 v/v) at −15 °C. Complex **2** was isolated as yellow crystals in 71% yield. The reaction was also performed by use of a Rayonet preparative photochemical reactor (Model RPR-208) with an RPR 350-nm lamp. The reaction time was 4 h, and the yield was determined to be 55% by ^1H NMR: mp 171–175 °C; ^1H NMR (CD_2Cl_2) δ 1.11 (m, 36, CH_3), 1.65 (m, 8, CH_2), 1.70 (m, 6, CH_2), 1.85 (m, 6, CH_2), 2.20 (m, 4, CH_2), 3.95 (d of d, 1, CHPh, $^3J_{PH}$ = 10.6 and 4.2 Hz), 7.30 (m, 18, Ph), 7.56 (d, 2, *o*-Ph, J = 7.00 Hz); $^{31}P\{^1H\}$ NMR ($CDCl_3$) δ 5.4, 8.4 (AB q, 2, trans-PEt_3, $^2J_{P(A)P(B)}$ = 406 Hz, $^1J_{PtP(A)} \approx {}^1J_{PtP(B)}$ = 2494 Hz), 2.8 (d, 1, PEt_3, $^1J_{PtP}$ = 3549 Hz, $^2J_{PP}$ = 3.6 Hz, $^4J_{PtP}$ = 98.6 Hz), −1.0 (d, 1, PEt_3, $^1J_{PtP}$ = 3690 Hz, $^2J_{PP}$ = 3.6 Hz, $^4J_{PtP}$ = 28.0 Hz); IR (KBr, cm^{-1}) ν(C≡C) 2108 (m). Anal. Calcd for $Pt_2C_{54}H_{81}P_4BF_4$: C, 48.73; H, 6.13; P, 9.31. Found: C, 48.93; H, 6.16; P, 9.10.

The preparation of ^{13}C-labeled **2** was performed by the procedure given above with use of the isotopically labeled derivative of **1** $[Pt_2(\mu\text{-}^{13}C{=}CHPh)(^{13}C{\equiv}CPh)(PEt_3)_4][BF_4]$ (**1**-$^{13}C_2$). This complex was prepared according to the published procedure with use of phenylacetylene-2-^{13}C.[12] The ^{13}C NMR spectra of **1**-$^{13}C_2$ and **2**-$^{13}C_2$ and the ^{31}P NMR spectra of **2** and **2**-$^{13}C_2$ are provided as supplementary material. Relevant NMR data are provided

(3) (a) Zipp, A. P. *Coord. Chem. Rev.* **1988**, *84*, 47–83. (b) Roundhill, D. M.; Gray, H. B.; Che, C.-M. *Acc. Chem. Res.* **1989**, *22*, 55–61.
(4) Casey, C. P.; Miles, W. H.; Fagan, P. J.; Haller, K. J. *Organometallics* **1985**, *4*, 559–563.
(5) Hughes, R. P.; Lambert, J. M. J.; Rheingold, A. L. *Organometallics*, **1985**, *4*, 2055–2057.
(6) (a) Bruce, M. I.; Hambley, T. W.; Liddell, M. J.; Snow, M. R.; Swincer, A. G.; Tiekink, E. R. T. *Organometallics* **1990**, *9*, 96–104. (b) Bruce, M. I.; Liddell, M. J.; Snow, M. R.; Tiekink, E. R. T. *Organometallics* **1988**, *7*, 343–350. (c) Bruce, M. I.; Hambley, T. W.; Snow, M. R.; Swincer, A. G. *Organometallics* **1985**, *4*, 501–508. (d) Bruce, M. I.; Hambley, T. W.; Snow, M. R.; Swincer, A. G. *Organometallics* **1985**, *4*, 494–500.
(7) Fischer, R. A.; Fischer, R. W.; Herrmann, W. A.; Herdweck, E. *Chem. Ber.* **1989**, *122*, 2035–2040.
(8) Benyunes, S. A.; Green, M.; McPartlin, M.; Nation, C. B. M. *J. Chem. Soc., Chem. Commun.* **1989**, 1887–1888.
(9) (a) Nesmeyanov, A. N.; Kolobova, N. E.; Zlotina, I. B.; Lokshin, B. V.; Leshcheva, L. F.; Znobina, G. K.; Anisimov, K. N. *J. Organomet. Chem.* **1976**, *110*, 339–344. (b) Nesmeyanov, A. N.; Aleksandrov, G. G.; Bokii, N. G.; Zlotina, I. B.; Struchkov, Yu. T.; Kolobova, N. E. *J. Organomet. Chem.* **1976**, *111*, C9–C12.
(10) (a) Drew, M. G. B.; Brisdon, B. J.; Brown, D. W.; Willis, C. R. *J. Chem. Soc., Chem. Commun.* **1986**, 1510–1512. (b) Brisdon, B. J.; Hodson, A. G. W.; Mahon, M. F.; Molloy, K. C. *J. Organomet. Chem.* **1988**, *344*, C8–C10.
(11) Lukehart, C. M.; McPhail, A. T.; McPhail, D. R.; Myers, J. B., Jr.; Soni, H. K. *Organometallics* **1989**, *8*, 1007–1014.
(12) Afzal, D.; Lenhert, P. G.; Lukehart, C. M. *J. Am. Chem. Soc.* **1984**, *106*, 3050–3052.

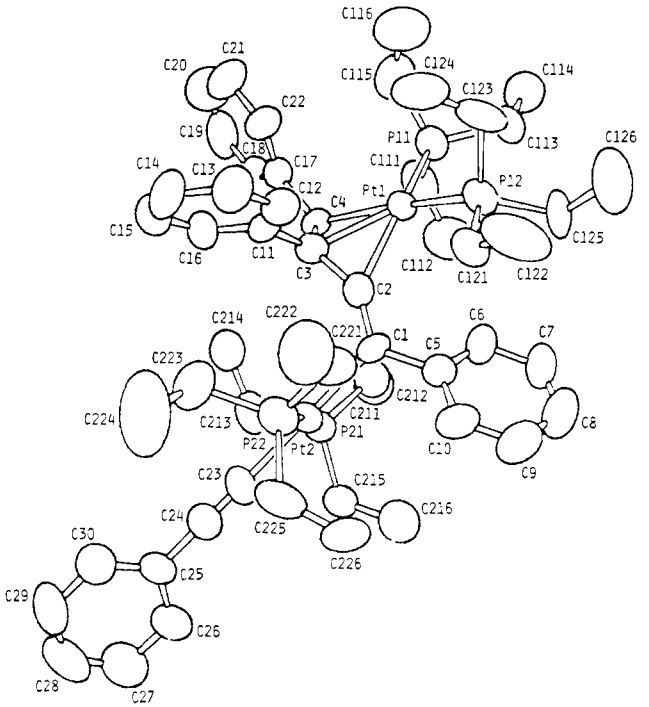

Figure 1. ORTEP diagram of the cationic portion of complex **2** showing the atomic numbering scheme. Hydrogen atoms have been omitted for clarity.

here (see text for the atom-labeling scheme). **1**-$^{13}C_2$: $^{13}C\{^1H\}$NMR ($CDCl_3$) δ 126–130 (spurious peaks due to phenyl carbon nuclei), 128.0 (m, $C{\equiv}CPh$, $^1J_{Pt(2)C}$ = 1038 Hz), 239.7 (d of m, $C{=}CHPh$, $^2J_{PC}$ = 8, 14, and 76 Hz, $^1J_{Pt(1)C}$ = 925 Hz, $^1J_{Pt(2)C}$ = 450 Hz). **2**-$^{13}C_2$: $^{13}C\{^1H\}$ NMR ($CDCl_3$) δ 100.3 ("t", C23, $^2J_{PC}$ = 14 Hz, $^1J_{Pt(2)C}$ = 917 Hz), 107.8 (s, C1, $^1J_{Pt(1)C}$ = 248 Hz), 125–131 (spurious peaks due to phenyl carbon nuclei), 160.5 (d, C2, $^2J_{PC}$ = 26 Hz, $^1J_{Pt(1)C}$ = 165 Hz, $^2J_{Pt(2)C}$ = 46 Hz); $^{31}P\{^1H\}$ NMR ($CDCl_3$) δ–1.0 (br s, P12, $^1J_{Pt(1)P}$ = 3690 Hz, $^4J_{Pt(2)P}$ = 28 Hz), 2.8 (br d and br s, P11, 70:30 isotopomer ratio, $^2J_{PC(2)}$ = 26 Hz, major isotopomer only, $^1J_{Pt(1)P}$ = 3549 Hz, $^4J_{Pt(2)P}$ = 98 Hz), 5.4 and 8.4 (d of AB quartets, P21 and P22, $^2J_{PP}$ = 406 Hz, $^2J_{PC(23)}$ = 14 Hz, $^1J_{Pt(2)P(A)} \approx {}^1J_{Pt(2)P(B)}$ = 249 Hz).

X-ray Crystal Structure Analysis of Complex 2. For X-ray measurements, a small crystal of **2** was mounted inside a thin-walled glass capillary. Crystallographic data collection parameters are summarized in Table I. Preliminary unit-cell parameters and space group information were derived from oscillation, Weissenberg, and precession photographs. Laue symmetry indicated that the space group was $P1$ or $P\bar{1}$, and it was shown to be the latter by structure solution and refinement. Intensity data were recorded on an Enraf-Nonius CAD-4 diffractometer (Cu Kα radiation, graphite monochromator; λ = 1.5418 Å). In addition to the usual Lorentz and polarization corrections, an empirical absorption correction was also applied to the intensity data.

The crystal structure was solved by the heavy-atom approach. Initial Pt atom coordinates were deduced from a Patterson map. A series of weighted F_o and difference Fourier syntheses, phased successively by an increasing number of non-hydrogen atoms, generated the complete structure of the complex cation. Several rounds of full-matrix least-squares adjustment of positional and thermal parameters (at first isotropic and subsequently anisotropic) followed. A difference Fourier synthesis then yielded coordinates for atoms of the tetrafluoroborate anion, which proved to be disordered over two orientations corresponding to inversion of the tetrahedral configuration at the boron atom. Continuation of the least-squares iterations ($\sum w\Delta^2$ minimized; $w = 1/\sigma^2(|F_o|)$, $\Delta = (|F_o| - |F_c|)$), which involved refinement of non-hydrogen atom positional and anisotropic temperature factor parameters (with hydrogen atoms included at their calculated positions), occupancy factors for a pair of fluorine atoms, and a secondary extinction correction, led to convergence at R = 0.040 (R_w = 0.046, GOF = 1.1). Final non-hydrogen atom positional parameters are listed in Table II. The solid-state conformation of the complex cation, with the atom-numbering scheme, is illustrated in Figure 1. Selected bond distances and angles are provided in Table III.

Table II. Final Non-Hydrogen Atomic Fractional Coordinates and Equivalent Isotropic Thermal Parameters for Complex 2 with Estimated Standard Deviations in Parentheses

atom	x	y	z	B_{eq}, Å^2
Pt(1)	0.45505 (3)	0.26120 (3)	0.22084 (4)	3.48 (1)
Pt(2)	0.16596 (3)	0.28290 (3)	0.33320 (4)	3.69 (1)
P(11)	0.6173 (2)	0.2743 (2)	0.2896 (3)	5.22 (9)
P(12)	0.3816 (2)	0.3251 (2)	0.0502 (3)	4.77 (8)
P(21)	0.2565 (2)	0.3338 (2)	0.5080 (3)	4.29 (8)
P(22)	0.0660 (2)	0.2227 (2)	0.1711 (3)	4.93 (9)
C(1)	0.2449 (7)	0.3137 (7)	0.2546 (8)	3.4 (3)
C(2)	0.3243 (7)	0.2603 (7)	0.2468 (9)	3.7 (3)
C(3)	0.3901 (7)	0.1819 (7)	0.2726 (9)	3.7 (3)
C(4)	0.4878 (7)	0.1829 (7)	0.3553 (9)	3.6 (3)
C(5)	0.2117 (8)	0.4035 (7)	0.2234 (9)	4.6 (3)
C(6)	0.2831 (9)	0.4472 (7)	0.2491 (10)	5.3 (4)
C(7)	0.2501 (11)	0.5308 (8)	0.2183 (11)	6.3 (4)
C(8)	0.1472 (12)	0.5684 (9)	0.1653 (12)	7.7 (5)
C(9)	0.0766 (11)	0.5258 (10)	0.1413 (12)	7.2 (5)
C(10)	0.1088 (9)	0.4428 (9)	0.1716 (11)	5.8 (4)
C(11)	0.3663 (7)	0.1032 (7)	0.2085 (10)	4.4 (3)
C(12)	0.3245 (9)	0.0964 (8)	0.0903 (10)	5.1 (4)
C(13)	0.2997 (10)	0.0237 (8)	0.0343 (11)	6.2 (4)
C(14)	0.3501 (9)	−0.0345 (8)	0.2091 (11)	5.4 (4)
C(15)	0.3105 (11)	−0.0412 (8)	0.0954 (12)	6.6 (5)
C(16)	0.3789 (8)	0.0386 (7)	0.2677 (11)	5.4 (3)
C(17)	0.5776 (7)	0.1074 (7)	0.3889 (10)	4.2 (3)
C(18)	0.6381 (9)	0.0977 (8)	0.5029 (11)	6.6 (4)
C(19)	0.7208 (10)	0.0277 (9)	0.5365 (13)	8.0 (5)
C(20)	0.7391 (10)	−0.0284 (10)	0.4570 (15)	8.5 (6)
C(21)	0.6819 (10)	−0.0210 (9)	0.3419 (15)	7.9 (5)
C(22)	0.5998 (8)	0.0483 (8)	0.3078 (12)	5.7 (4)
C(23)	0.0878 (8)	0.2553 (7)	0.4122 (10)	4.7 (3)
C(24)	0.0476 (8)	0.2375 (7)	0.4548 (10)	4.6 (3)
C(25)	−0.0006 (7)	0.2151 (8)	0.5164 (9)	4.7 (3)
C(26)	−0.0409 (9)	0.2740 (9)	0.5866 (12)	6.7 (4)
C(27)	−0.0864 (11)	0.2480 (10)	0.6406 (12)	7.5 (5)
C(28)	−0.0971 (10)	0.1701 (10)	0.6274 (12)	8.3 (5)
C(29)	−0.0599 (11)	0.1124 (9)	0.5555 (14)	8.8 (5)
C(30)	−0.0154 (10)	0.1357 (9)	0.5008 (13)	7.5 (5)
C(111)	0.6540 (9)	0.3074 (9)	0.4449 (11)	6.4 (4)
C(112)	0.5886 (12)	0.3852 (11)	0.4698 (14)	9.2 (6)
C(113)	0.6397 (8)	0.3551 (8)	0.2320 (11)	5.9 (4)
C(114)	0.7413 (10)	0.3684 (9)	0.2884 (15)	8.1 (5)
C(115)	0.7199 (10)	0.1850 (9)	0.2964 (15)	7.7 (5)
C(116)	0.7160 (12)	0.1487 (11)	0.1808 (15)	9.9 (6)
C(121)	0.2510 (9)	0.3249 (8)	−0.0254 (10)	5.5 (4)
C(122)	0.1999 (11)	0.3493 (14)	−0.1457 (12)	10.3 (7)
C(123)	0.4422 (9)	0.2649 (11)	−0.0439 (10)	7.3 (5)
C(124)	0.4410 (12)	0.1730 (11)	−0.0664 (12)	9.1 (6)
C(125)	0.3813 (10)	0.4339 (8)	0.0496 (10)	6.3 (4)
C(126)	0.3770 (15)	0.4620 (11)	−0.0564 (14)	11.7 (7)
C(211)	0.3552 (9)	0.3776 (8)	0.5205 (10)	4.9 (4)
C(212)	0.4170 (10)	0.4054 (9)	0.6409 (12)	6.5 (4)
C(213)	0.3176 (9)	0.2541 (8)	0.6126 (9)	5.4 (4)
C(214)	0.3931 (10)	0.1810 (9)	0.5854 (11)	6.6 (4)
C(215)	0.1757 (8)	0.4160 (8)	0.5634 (10)	5.5 (4)
C(216)	0.1172 (11)	0.4898 (10)	0.4861 (12)	7.4 (5)
C(221)	0.0758 (9)	0.2344 (9)	0.0422 (10)	5.9 (4)
C(222)	0.0215 (13)	0.1832 (11)	−0.0674 (12)	8.9 (6)
C(223)	0.0972 (11)	0.1103 (8)	0.1910 (14)	7.3 (5)
C(224)	0.0226 (16)	0.0677 (13)	0.1582 (25)	17 (1)
C(225)	−0.0669 (8)	0.2647 (9)	0.1409 (11)	6.2 (4)
C(226)	−0.1058 (10)	0.3568 (10)	0.1292 (13)	8.8 (5)
F(1)	0.3947 (10)	0.7609 (7)	0.2133 (16)	23.7 (8)
F(2)	0.3498 (13)	0.6489 (8)	0.1351 (16)	24.0 (9)
F(3)[a]	0.3179 (14)	0.7363 (14)	0.0374 (18)	17.5 (8)
F(4)	0.2459 (12)	0.7681 (16)	0.1327 (18)	28 (1)
F(3')[b]	0.3283 (21)	0.7153 (19)	0.2487 (27)	17 (1)
B	0.3319 (18)	0.7307 (16)	0.1445 (21)	11.0 (8)

[a] Occupancy factor 0.64. [b] Occupancy factor 0.36.

For structure factor calculations, neutral atom scattering factors and their anomalous dispersion corrections were taken from ref 13. Crystallographic calculations were performed on PDP11/44

Table III. Selected Interatomic Distances (Å) and Angles (deg) for Complex 2 with Estimated Standard Deviations in Parentheses

(a) Bond Distances

Pt(1)-P(11)	2.327 (3)	C(1)-C(2)	1.29 (1)
Pt(1)-P(12)	2.315 (4)	C(1)-C(5)	1.51 (2)
Pt(1)-C(2)	2.17 (1)	C(2)-C(3)	1.38 (1)
Pt(1)-C(3)	2.23 (1)	C(3)-C(4)	1.43 (1)
Pt(1)-C(4)	2.18 (1)	C(3)-C(11)	1.50 (2)
Pt(2)-P(21)	2.294 (3)	C(4)-C(17)	1.51 (1)
Pt(2)-P(22)	2.313 (3)	C(23)-C(24)	1.11 (2)
Pt(2)-C(1)	2.10 (1)	C(24)-C(25)	1.45 (2)
Pt(2)-C(23)	2.07 (2)		

(b) Bond Angles

P(11)-Pt(1)-P(12)	101.9 (1)	Pt(2)-C(1)-C(5)	116 (1)
P(11)-Pt(1)-C(2)	151.2 (3)	C(2)-C(1)-C(5)	123 (1)
P(11)-Pt(1)-C(3)	131.3 (2)	Pt(1)-C(2)-C(1)	138 (1)
P(11)-Pt(1)-C(4)	94.1 (3)	Pt(1)-C(2)-C(3)	74 (1)
P(12)-Pt(1)-C(2)	101.3 (3)	C(1)-C(2)-C(3)	146 (1)
P(12)-Pt(1)-C(3)	125.1 (3)	Pt(1)-C(3)-C(2)	69 (1)
P(12)-Pt(1)-C(4)	162.6 (3)	Pt(1)-C(3)-C(4)	69 (1)
C(2)-Pt(1)-C(3)	36.6 (4)	Pt(1)-C(3)-C(11)	124 (1)
C(2)-Pt(1)-C(4)	65.8 (3)	C(2)-C(3)-C(4)	114 (1)
C(3)-Pt(1)-C(4)	37.9 (3)	C(2)-C(3)-C(11)	123 91)
P(21)-Pt(2)-P(22)	171.5 (2)	C(4)-C(3)-C(11)	122 (1)
P(21)-Pt(2)-C(1)	93.2 (2)	Pt(1)-C(4)-C(3)	73 (1)
P(21)-Pt(2)-C(23)	85.9 (3)	Pt(1)-C(4)-C(17)	122 (1)
P(22)-Pt(2)-C(1)	95.1 (2)	C(3)-C(4)-C(17)	125 (1)
P(22)-Pt(2)-C(23)	85.8 (3)	Pt(2)-C(23)-C(24)	177 (1)
C(1)-Pt(2)-C(23)	178.7 (3)	C(23)-C(24)-C(25)	177 (1)
Pt(2)-C(1)-C(2)	120 (1)		

and MicroVAX computers by use of the Enraf-Nonius Structure Determination Package (SDP).

Results and Discussion

The reaction of the cationic diplatinum μ-phenylethenylidene complex **1** with a nearly stoichiometric amount of diphenylacetylene under photolysis gives the cationic diplatinum μ-η^1:η^3-butadienediyl complex **2** in 71% yield, as shown in eq 1. The identity of compound **2**

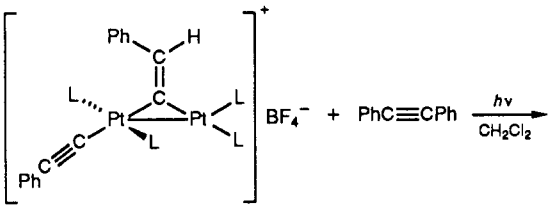

1, L = PEt_3

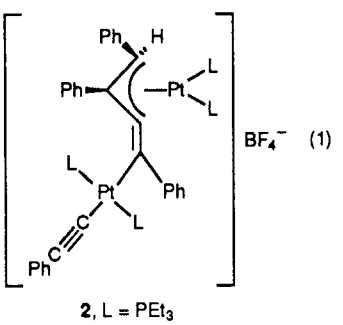

2, L = PEt_3

indicates that diphenylacetylene has been successfully incorporated into complex **1** via C–C bond coupling with the μ-phenylethenylidene ligand. This coupling increases the complexity of the unsaturated hydrocarbyl ligand that bridges the two metal centers and represents an unprecedented route to the formation of butadienediyl complexes.

Furthermore, the incorporation of diphenylacetylene into **1** to form **2** must be accompanied by an unusual rearrangement of both the two metal centers and the μ-phenylethenylidene ligand. Photochemical reaction of diiron μ-alkenylidene complexes with diazo compounds or alkynes as reported by Casey and co-workers proceeds by overall insertion reactivity.[4,14] The formation of **2**, however, apparently proceeds by an overall rearrangement of the Pt–C, C–C or C–H connectivity of the original μ-phenylethenylidene ligand. A control reaction demonstrates that complex **1** and diphenylacetylene do not react thermally in CH_2Cl_2 solution at 25 °C over 72 h.

The spectroscopic data of complex **2** are consistent with the structure shown. In the IR spectrum, the C–C triple-bond stretching vibration for the phenylacetylide ligand appears as a band at 2108 cm^{-1}. In the ^1H NMR spectrum, the resonance for the unique allyl proton appears at δ 3.95 as a doublet of doublets with $^3J_{PH}$ coupling constants of 10.6 and 4.2 Hz. Peak broadening due presumably to underlying Pt satellite resonances indicates possible $^2J_{PtH}$ coupling of less than 25 Hz. These NMR data are consistent with those of other anti allyl protons in (η^3-allyl)platinum phosphine compounds.[15] The presence of this allyl resonance is a diagnostic indication of the formation of a butadienediyl complex from **1**. In the ^{31}P NMR spectrum of **2**, the two phosphorus nuclei of the PtL_2^+ fragment are nonequivalent, as anticipated, and undergo coupling with the expected small $^2J_{PP}$ coupling constant of 3.6 Hz. Because of the dissymmetry generated by the (η^3-butadienediyl)PtL_2^+ moiety, the two trans PEt_3 ligands are also symmetry-nonequivalent. These phosphorus nuclei couple to give an AB quartet resonance with a $^2J_{PP}$ coupling constant of 406 Hz, which is consistent with a trans geometry at the second platinum center.

The constitution of **2** has been determined by X-ray crystallography. An ORTEP diagram of the cationic portion of **2** showing the atomic numbering scheme is given in Figure 1. Selected interatomic distances and angles of **2** are listed in Table III. The X-ray results confirm the presence of an η^1:η^3-butadienediyl ligand bridging between two separated Pt moieties. The cation consists formally of two organometallic moieties, viz. (η^3-allyl)PtL_2^+ and neutral *trans*-PtL_2(C≡CPh)(η^1-alkenyl) fragments, each of which has the expected structural features such as Pt(1)–C(allyl) distances of 2.17 (1), 2.23 (1), and 2.18 (1) Å and a Pt(2)–C(alkenyl) distance of 2.07 (2) Å. The terminal phenylacetylide ligand has a C–C triple-bond length of 1.11 (2) Å. The skeleton of the butadienediyl ligand has the following structural features: (1) typical C(allyl)–C(allyl) distances of 1.38 (1) and 1.43 (1) Å, (2) and *exo*-alkylidene C(1)–C(2) distance of 1.29 (1) Å, which represents an essentially unperturbed C–C double bond, (3) a central angle of 114 (1)° within the allyl portion, (4) a C(1)–C(2)–C(3) angle of 146 (1)° between the *exo*-alkylidene bond vector and the adjacent allyl C–C bond vector, and (5) angles around the *exo*-alkylidene carbon, C(1), of 120 (1)°, 116 (1)°, and 123 (1)°, indicating a planar (and nearly sp^2) hybridization at this atom.

The mechanism of formation of complex **2** remains undetermined. From the structure of **2**, one might suggest that the C(3)PhC(4)Ph and C(2)C(1)Ph fragments are derived from the diphenylacetylene reagent and the μ-alkenylidene ligand of **1**, respectively. Such a reaction would require considerable rearrangement of the C–H and

(13) *International Tables for X-ray Crystallography*; Kynoch: Birmingham, U.K., 1976; Vol. IV.

(14) (a) Casey, C. P.; Austin, E. A. *Organometallics* **1986**, *5*, 584–585. (b) Casey, C. P.; Austin, E. A. *J. Am. Chem. Soc.* **1988**, *110*, 7106–7113.

(15) Clark, H. C.; Hampden-Smith, M. J.; Rüegger, H. *Organometallics* **1988**, *7*, 2085–2093.

Pt–C or C–Ph connectivity of the μ-phenylethenylidene ligand. A hydrogen atom shift would be required. Several types of hydrogen shifts have been identified in reactions of alkynes at mononuclear electron-rich metal centers.[16]

To probe the mechanism of formation of complex **2**, we prepared the ^{13}C-labeled derivative of **1** $[Pt_2(\mu\text{-}^{13}C{=}CHPh)(^{13}C{\equiv}CPh)(PEt_3)_4][BF_4]$ (**1**-$^{13}C_2$) and reacted it with diphenylacetylene under photolysis to give the isotopically labeled product **2**-$^{13}C_2$. In the ^{13}C NMR spectrum of **1**-$^{13}C_2$, the alkynyl carbon resonance appears at δ 128.0 with $^1J_{PtC}$ coupling of 1038 Hz. The complex fine structure of this resonance indicates that all other coupling is probably below 15 Hz. These data are consistent with those reported for related *trans*-$PtL_2(C{\equiv}CPh)_2$ compounds.[17] The ^{13}C resonance for the μ-alkenylidene carbon nucleus appears at δ 239.7 and shows the following major couplings: $^2J_{PC}$ = 76, 14, and ca. 8 Hz and $^1J_{PtC}$ = 925 and 450 Hz.

Within the assumption that $^2J_{CC}$ coupling through a Pt center is less than ca. 10 Hz and the recognition that spectral resolution is less than ca. 10 Hz, the ^{13}C and ^{31}P NMR data of **2**-$^{13}C_2$ can be interpreted as a mixture of isotopomers **3** and **4** in a ratio of ca. 70:30, respectively.

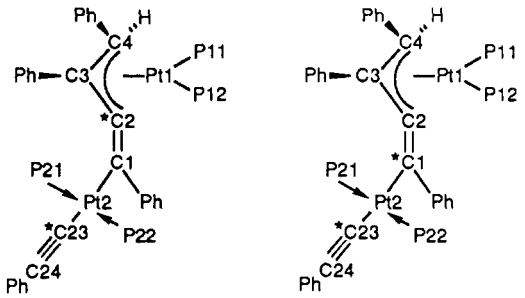

3 (70%) **4** (30%)

The major spectral features that support this conclusion are as follows. (1) The AB quartet pattern for the resonance of the P21 and P22 nuclei in the ^{31}P NMR spectrum of **2** is split into a doublet of AB quartets in the corresponding spectrum of **2**-$^{13}C_2$ due to the full incorporation of a ^{13}C label at C23 ($^2J_{PC(23)}$ = 14 Hz). (2) The phosphorus spectrum of **2**-$^{13}C_2$ shows the indicated isotopomeric mixture most clearly in the resonance of nucleus P11 (or P12, whichever nucleus is trans to C2). Although spectral resolution is too low to reveal the expected $^2J_{PP}$ coupling as observed in the corresponding spectrum of **2**, this resonance consists of a central peak at δ 2.8 assigned to isotopomer **4**, where a ^{13}C label is not present at C2, and of two flanking peaks assigned to isotopomer **3**, in which a ^{13}C label is present at C2. An isotopomer mixture of 70:30 (3:4) is estimated from the relative intensities of these peaks. The value of the $^2J_{PC(2)}$ coupling in **3** is 26 Hz. (3) The ^{13}C NMR data for **2**-$^{13}C_2$ support this assignment. A "triplet" resonance at δ 100.3 with $^2J_{PC}$ coupling of 14 Hz is assigned to C23, while the resonance of the C2 nucleus of **3** appears as a doublet at δ 160.5 with $^2J_{PC}$ coupling of 26 Hz (including additional coupling to *both* Pt nuclei). (4) Although the location of the remaining 30% of one ^{13}C label is less certain, we assign this label to C1 of **4**.[18] A singlet resonance at δ 107.8 in the ^{13}C NMR spectrum of **2**-$^{13}C_2$ is consistent with this assignment because both $^2J_{CC}$ and $^2J_{PC}$ coupling might well be less than ca. 10 Hz and, therefore, not resolved. In addition, coupling to only one Pt nucleus (of 248 Hz) is observed for this resonance. Presumably, $^2J_{PtC1}$ coupling to Pt1 is very small because of the π-bonding of the allyl ligand to Pt1. In isotopomer **3**, $^1J_{Pt1C}$ coupling is only 165 Hz.

Although a specific mechanism for the formation of **2** cannot be determined conclusively from an analysis of the spectroscopic data of **2**-$^{13}C_2$, these data indicate that a complex rearrangement, probably involving at least one branching point, does occur. Isotopomer **3** must be formed via a rearrangement of the Pt–C(alkenylidene) bonding of **1** and with a hydrogen migration. Formation of isotopomer **4** must involve a similar hydrogen migration and overall migration of the alkenylidene phenyl group. Both isotopomers are formed presumably by incorporation of the intact diphenylacetylene molecule as the PhC(3)C(4)Ph fragment of the μ-η^1:η^3-butadienediyl ligand through C–C coupling. We currently favor photochemical activation of **1** to a long-lived excited state[2] that then is quenched by diphenylacetylene, probably through [2 + 2] cycloaddition or organometallic insertion reactions. Further definition of the mechanism of this reaction might be possible if this reaction can be extended to other alkynes and to other derivatives of complex **1**.

Acknowledgment. C.M.L. thanks the donors of the Petroleum Research Fund, administered by the American Chemical Society, for support of this research. A loan of platinum metal from Johnson Matthey, Inc., is gratefully acknowledged. We thank Ms. M. D. Owen for her assistance in acquiring ^{13}C NMR data.

Supplementary Material Available: Tables of crystal data, non-hydrogen atom fractional coordinates, anisotropic temperature factors, hydrogen atom fractional coordinates, interatomic distances and angles, torsion angles, and equations of least-squares planes for complex **2**, ^{13}C NMR spectra of **1**-$^{13}C_2$ and **2**-$^{13}C_2$, and ^{31}P NMR spectra of **2** and **2**-$^{13}C_2$ (23 pages); a listing of observed and calculated structure factors for complex **2** (31 pages). Ordering information is given on any current masthead page.

(16) Pombeiro, A. J. L. *J. Organomet. Chem.* **1988**, *358*, 273–282.
(17) Sebald, A.; Wrackmeyer, B. *Z. Naturforsch.* **1985**, *40B*, 1481–1484.
(18) Musco, A.; Pontellini, R.; Grassi, M.; Sironi, A.; Meille, S. V.; Rüegger, H.; Ammann, C.; Pregosin, P. S. *Organometallics* **1988**, *7*, 2130–2137.